Can Ionic Liquids be used as Templating Agents for Controlled Design of Uranium-containing Nanomaterials?

Ann E. Visser,[a*] Nicholas J. Bridges,[a] and Michael H. Tosten[a]

[a] Savannah River National Laboratory, Aiken, SC 29808

[*] ann.visser@srnl.doe.gov

803-725-5383

Abstract

Nanostructured uranium oxides have been prepared in ionic liquids as templating agents. Using the ionic liquids as reaction media for inorganic nanomaterials takes advantage of the pre-organized structure of the ionic liquids which in turn controls the morphology of the inorganic nanomaterials. Variation of ionic liquid cation structure was investigated to determine the impact on the uranium oxide morphologies. For two ionic liquid cations, increasing the alkyl chain length increases the aspect ratio of the resulting nanostructured oxides. Understanding the resulting metal oxide morphologies could enhance fuel stability and design.

Keywords

Inorganic compounds, nanostructures, oxides, X-ray diffraction

1. Introduction

Ionic Liquids (ILs) are a class of solvents with ionic character and have been found to be useful, or at least produce unexpected and interesting results, in many aspects of scientific research. The use of ILs in synthesis of inorganic nanostructured materials is a relatively new application. One of the direct benefits of using ILs in low temperature synthesis of metal oxides is that these materials provide a solvation environment completely different from aqueous or ordinary organic solvents that are more commonly used in the synthesis. The recent developments in the use of ILs as reaction media take advantage of the structure of the ILs to template porous inorganic nanomaterials,[1, 2] iridium and gold nanoparticles,[3] titanium dioxide nanocrystals,[4] mesoporous silica,[5] and cobalt-platinum nanorods.[6] It is proposed that the intrinsic high charge and polarizability of the IL creates an electrostatic and steric stabilization for nanoparticles.

The uranium oxide systems have been heavily studied due to their use in commercial fuel fabrication. In aqueous solutions, the U(VI) oxidation state predominates the chemistry through the stabilizing trans-oxo ligands forming the uranyl cation UO_2^{2+}. In the solid state there is minimal energy difference between the IV and VI oxidation states; hence, both oxidation states are present in U_3O_8.[7] Most uranium oxides, especially on the scale required for nuclear fuel manufacture, are prepared by calcination and sintering of uranium-bearing material (e.g., uranyl oxalate, uranyl nitrate hexahydrate, etc.). The preferred uranium oxide system for nuclear fuels is UO_2 as it has the highest fissile density of the oxide matrices. Other uranium oxide systems (e.g., U_3O_8 and UO_3) can be prepared, although their use in fuel fabrication is generally avoided due to less favorable fissile densities.

In addition to nuclear fuel, other applications for uranium oxides include reactions with organic compounds (e.g., acetaldehyde),[8] desulfurization,[9] and selective reduction of nitrogen oxide (NO).[10]

Uranium oxides nanoparticles exhibit numerous compositions and morphologies as revealed by new synthesis methods including electrochemical deposition,[11] self-assembly in porous host matrices,[12] and hydrothermal synthesis.[13] Thus, the interest in developing new methods for preparing uranium oxides stems from both the use of new particle morphologies for nuclear fuel fabrication, and in catalysis where templating reaction media could also be used.

Here, we use 1-octyl-3-methylimidazolium tetrafluoroborate and 1-dodecyl-3-methylimidazolium tetrafluoroborate in the synthesis of uranium oxide nanoparticles. Using relatively low reaction temperatures, uranium oxide products with different morphologies were obtained and highlight the versatility of the synthesis route.

2. Materials and Methods

2.1 Chemicals

All ionic liquids were used as received from IoLiTec (Tuscaloosa, AL). Reagent grade depleted uranyl acetate dihydrate (Merck) was used without additional purification. All other chemicals were used as received from Sigma Aldrich, and used as received.

2.2 Oxide Synthesis

Uranyl acetate dihydrate, ionic liquid, and sodium hydroxide were weighed and subsequently ground using a mortar and pestle. The mole ratio of uranyl acetate dihydrate to sodium hydroxide was 1:2. The mole ratio of uranyl acetate dihydrate to the IL was 1:3.5. Each mixture was transferred into an open top glass vial and placed in a vented reaction vessel. The reaction vessel was closed and heated via heat tape wrapped around the outside of the vessel. The samples were heated to 150 ^{o}C for 48 hours. During the synthesis, the headspace was constantly purged by flowing air through the vessel. After 48 hours, the samples cooled to room temperature and were subsequently washed with water and isopropanol.

2.3 Characterization and instrumentation

Powder XRD analyses were performed with Bruker D8 Advance powder X-ray diffractometer. Samples for TEM analysis were prepared by placing a small amount of product in a glass vial and adding 8 mL of 2 wt % sodium dodecyl sulfate in water. The solutions were sonicated for 15 seconds to disperse the solids within the solution. A drop of the sonicated solution was placed on a 3 mm copper grid and the water allowed to evaporate. TEM analysis was performed using a JEOL 2010 JEM transmission electron microscope operating at 200 kV.

3. Results

Syntheses were performed using two different ILs; 1-octyl-3-methylimidazolium tetrafluoroborate ([C_8mim][BF_4]) and 1-dodecyl-3-methylimidazolium tetrafluoroborate ([C_{12}mim][BF_4]). Bulk powder XRD analysis of the product from the [C_8mim][BF_4]

synthesis corresponded to sodium uranium oxide hydrate ($Na_2U_2O_7$•$6H_2O$). The electron diffraction pattern acquired during TEM analysis of individual particles identified UO_2. Product morphologies were determined using TEM and elemental composition determined using electron dispersive spectroscopic analysis. Figure 1 shows TEM images and electron diffraction patterns of uranium oxide products from synthesis with ([C_8mim][BF_4]). Nanoparticles in both A and A2 are composed of U and O. In A, the particles are 50 – 300 nm wide and 100 – 700 nm in length and the electron diffraction pattern is a close match with UO_2 (cubic, $a_o = 5.47$Å). The diffraction pattern from the solids in A2, also identified as UO_2, is shown in A2-1.

Figure 2 shows the TEM images for the products obtained from synthesis using [C_{12}mim][BF_4]. The solids contain uranium and oxygen. Bulk XRD analysis of the products revealed sodium diuranate. However, TEM identified both UO_2 and amorphous solids. The rods are amorphous and show no spots in the electron diffraction pattern (B-1). The TEM image in Figure 2 part B2 is the minor product from the [C_{12}mim][BF_4] synthesis. The electron diffraction pattern (B2-1) reveals the solid to be cubic UO_2.

4. Discussion

The liquid structure of the ILs has been postulated to be micro-structured with polar and nonpolar regions with hydrogen-bonded networks.[14] One of the most widely studied IL families contains the 1-alkyl-3-methylimidazolium cation in combination with the hexafluorophosphate anion. The IL cations are composed of a polar aromatic head group, where most of the electrostatic charge is located, and a nonpolar alkyl side chain.

Neutron scattering results from 1-alkyl-3-methylimidazolium hexafluorophosphate ILs show anions and charge-bearing imidazolium cations associated through Coulombic attraction and the anions are located above and below the imidazolium ring.[15] Changing the length of the alkyl chain on the imidazolium cation has little effect on the coordination environment around the IL cation or anion.[15] Although the neutron diffraction results do not necessarily support an alkyl chain dominated aggregation to form alkyl-chain channels in the 1-alkyl-3-methylimidazolium hexafluorophosphate ILs, fluorescence data supports selective solvation of fluorescent probe molecules in the hydrophobic region of an 1-alkyl-3-methylimidazolium bis(trifluoromethylsulfonyl)imide IL and some degree of alkyl chain alignment.[16]

Bulk analysis vs. single particle analysis provided different answers regarding product composition. Although samples were washed with water and isopropanol before XRD analysis, TEM samples were further "washed" by sonicating in water with a surfactant. Furthermore, the sample could have dehydrated in the low vacuum used in TEM analysis.

From TEM analysis, the oblong UO_2 nanoparticles comprise the majority of the product formed from the reaction in $[C_8mim][BF_4]$. In addition to the individual UO_2 nanoparticles in Figure 1 (A), star shaped crystals (A2) were grown from multiple nucleation sites. Both the oblong and star-shaped solids were present in the product. The disk and rods grown from $[C_{12}mim][BF_4]$ suggest different growth mechanisms, especially since the rods are amorphous and the disk is UO_2.

In comparison to the synthesis of zinc oxide in 1-alkyl-3-methylimidazolium-based ILs, the UO_2 products have very small aspect ratios.[17, 18] Zinc oxide nanorods prepared in 1-ethyl, 1-butyl, 1-hexyl, and 1-octyl substituted 1-alkyl-3-methylimidazolium ILs have an aspect ratio that decreases from nominally 40 to 5 as the alkyl chain length increases. With the octyl and dodecyl substituted ILs used here, the decreasing aspect ratio trend continues and the uranium oxide products are essentially two dimensional. Although the rod-shaped nanoparticles contain U, they are likely a byproduct of the synthesis reaction.

A proposed growth mechanism for uranium dioxide in [C_8mim][BF_4] and [C_{12}mim][BF_4] likely involves direct interaction with the IL cation.[19] The oblong, star, and disk-shaped nanoparticles are formed in ionic regions within the IL, likely via oxygen interacting with the C-2 proton on the imidazolium ring. Other metal oxides have been prepared in ILs and FTIR analysis shows interaction between the H-C at the C-2 position on the imidazolium ring and a corresponding weakening in the H-C stretching vibration band.[20] Considering the basicity of the IL-NaOH mixtures, the mechanism for UO_2 formation in these ILs could involve formation of a carbene intermediate. Further decomposition of the carbene intermediate would provide a reducing atmosphere and keep UO_2 from oxidizing to form UO_3 or U_3O_8.[19]

5. Conclusions

Uranium oxides nanostructures from ellipse- to disk- to star-shaped have been successfully prepared in ILs using a low temperature synthesis route. The structure of the IL utilized in these syntheses has little impact on the final product, possibly due to the use of ILs with long alkyl chains. These initial results show the utility of ILs as a novel route for actinide oxide preparation. Further work to optimize the synthesis parameters is warranted.

Acknowledgements

This project was funded through the SRNL Laboratory Directed Research and Development program. This manuscript has been authored by Savannah River Nuclear Solutions, LLC under Contract No. DE-AC09-08SR22470 with the U.S. Department of Energy. The United States Government retains and the publisher, by accepting this article for publication, acknowledges that the United States Government retains a non-exclusive, paid-up, irrevocable, worldwide license to publish or reproduce the published form of this work, or allow others to do so, for United States Government purposes

References

[1] H. S. Park, Y. S. Choi, Y. J. Kim, W. H. Hong, H. Song, Ad. Funct. Mater., 17 (2007) 2411.

[2] J. Lian, X. Duan, J. Ma, P. Peng, T. Kim, W. Zheng, ACS Nano, 3 (2009) 3749.

[3] J. Dupont, G. S. Fonseca, A. P. Umpierre, P. F. P. Fichtner, S. R. Teixeira, JACS, 124 (2002) 4228.

[4] Y. Zhou, M. Antonietti, JACS, 125 (2003) 14960.

[5] Y. Zhou, J.H. Schattka, M. Antonietti, Nano Lett., 4 (2004) 477.

[6] Y. Wang, H. Yang, JACS, 127, (2005) 5316.

[7] R. J. M. Konings, L.R. Morss, J. Fuger, in: L. R. Morss, N. M. Edelstein, J. Fuger (Eds.), Chemistry of the Actinide Elements, Springer: Dordrecht, 2006, 2131.

[8] H. Madhavaram, H. Idriss, J. Catal., 224 (2004) 358.

[9] T. W. Schlereth, M. N. Medhili, B. V. Yakshinskiy, T. Gouder, T. E. Madey, J. Phys. Chem. B, 109 (2005) 20895.

[10] T. Campbell, M. A. Newton, V. Boyd, D. F. Lee, J. Evans, J. Phys. Chem. B, 109 (2005) 2885.

[11] G. Rousseau, M. Fattahi, B. Grambow, L. Desgranges, F. Boucher, G. Ouvrard, N. Millot, J. C. Niepce, J. Solid State Chem., 182 (2009) 2591.

[12] D. Kumar, S. Bera, A. K. Tripathi, G. K. Dey, N. M. Gupta, Microporous Mesoporous Mater., 66 (2003) 157.

[13] Q. Wang, G.-D. Li, S. Yu, J.-L. Li, J.-S. Chen, J. Mater. Chem., 18 (2008) 1146.

[14] J. N. A. Canongia Lopes and A. A. H. Padua, J. Phys. Chem. B, 110 (2006) 3330.

[15] C. Hardacre, J. D. Holbrey, C. L. Mullan, T. G. A. Youngs, D. T. Bowron, J. Chem. Phys., 133 (2010) 74510.

[16] K. Fruchey, M. D. Fayer, J. Phys. Chem. B, 114 (2010) 2840.

[17] L. Wang, L.-X. Chang, L.-Q. Qiang, S.-Z. Xu, M.-H. Zeng, S.-L. Pan, J. Mater. Chem., 21 (2011) 15732.

[18] L. Wang, L. Chang, B. Zhao, Z. Yuan, G. Shao, W. Zheng, Inorg. Chem. 47 (2008) 1443.

[19] M. Swadzba-Kwasny, L. Chancelier, S. Ng, H. G. Manyar, C. Hardacre, P. Nockemann, Dalton Trans., 41 (2012) 219.

[20] J. J. Wang, S. Zhang, H. Wang, Y. Pei, J. Chem. Eng. Data, 54 (2009) 3252.

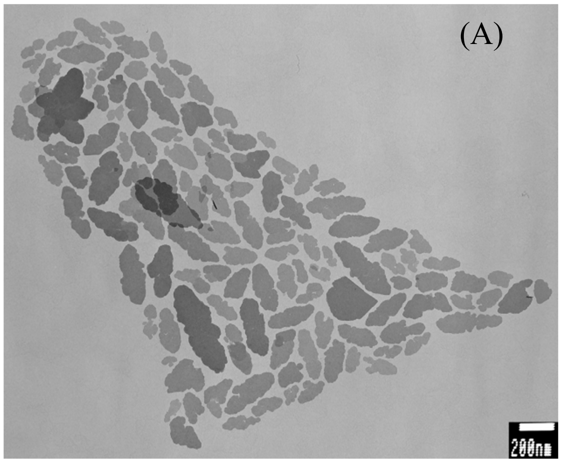
(A)
200nm

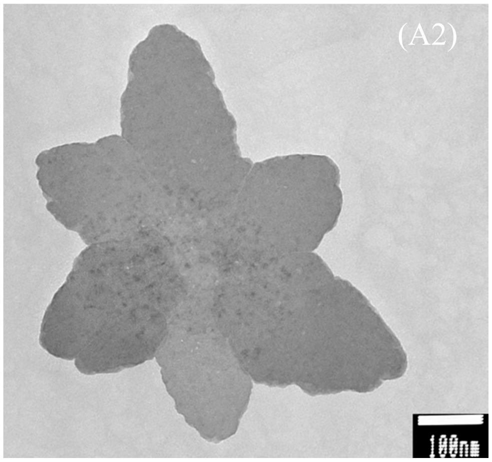
(A2)
100nm

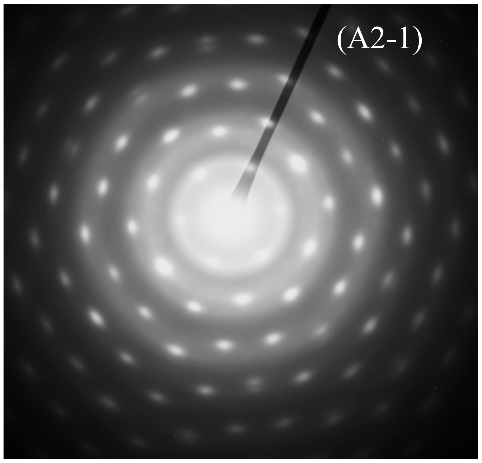
(A2-1)

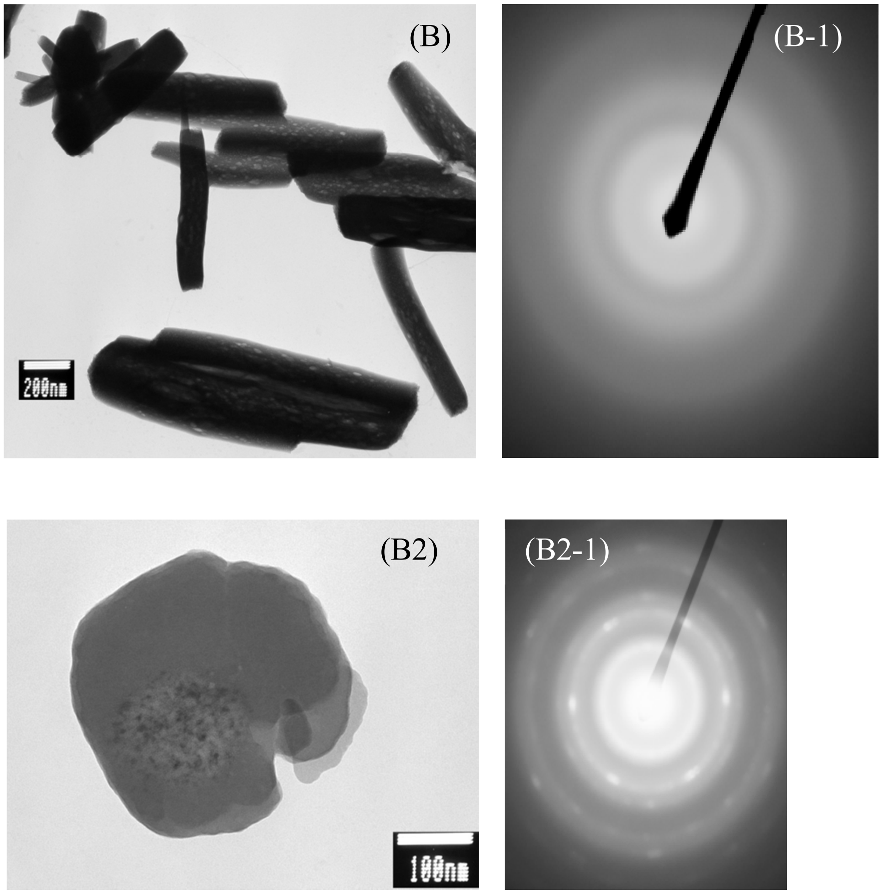
(B)
200nm
(B-1)
(B2)
100nm
(B2-1)

Figure 1: TEM Images (A, A2) and Electron Diffraction Pattern for Uranium Oxide Synthesized in [C_8mim][BF_4] (A2-1).

Figure 2: TEM Images (B, B2) and Electron Diffraction (B-1, B2-1) for Uranium Oxide Synthesized in [C_{12}mim][BF_4].